Journal of Power Sources 209 (2012) 30–39

Contents lists available at SciVerse ScienceDirect

Journal of Power Sources

journal homepage: www.elsevier.com/locate/jpowsour

Research on a battery test profile based on road test data from hybrid fuel cell buses

Xuning Feng, Jianqiu Li, Languang Lu, Jianfeng Hua, Liangfei Xu, Minggao Ouyang*

State Key Laboratory of Automotive Safety and Energy, Tsinghua University, Beijing 100084, PR China

ARTICLE INFO

Article history:
Received 31 August 2011
Received in revised form 16 February 2012
Accepted 20 February 2012
Available online 3 March 2012

Keywords:
Battery test profile
Hybrid fuel cell bus
Practical operating conditions
Charge/discharge(C/D) current
"Three-Ridge" map

ABSTRACT

To promote the performance of the batteries used in hybrid vehicles, an effective test profile is needed. A test profile could also improve the efficiency of battery development research efforts. This paper proposes a test profile for battery equivalence research, which can accurately simulate practical operating conditions and make inconsistency among batteries. The proposed test profile is based on practical data acquired from the hybrid Polymer Electrolyte Membrane (PEM) fuel cell buses demonstrated at the 2010 Shanghai World Expo. The control strategy of the demonstration buses is first explained, followed by presentation of maps of the acquired data. Using the maps, the practical conditions are discussed. Importantly, a "Three-Ridge" map style is proposed by analyzing the current density statistics. Additionally, a fast Fourier transform (FFT) analysis of the battery current is adopted to find the conversion frequency of the current in practical conditions. Based on these analyses, a credible battery test profile for hybrid PEM fuel cell buses is proposed. Finally, an experiment verifies that the proposed test profile can simulate the practical operating conditions of a hybrid vehicle battery pack.

1. Introduction

By employing a battery, the hybrid electric vehicle has many advantages [1,2]. For example, the battery can help the primary power source, e.g., an internal combustion engine or a fuel cell, work in its high efficiency range in order to reduce energy consumption [1–3]. To do so, energy is taken from the battery when the power requirements exceed those that can be provided by the primary power source, and energy is stored in the battery when the power requirements are low [3–5].

Currently, Li-ion batteries are favored by researchers as a promising auxiliary power source for hybrid vehicles, for their high power density, high accessible discharge rate and many other desirable characteristics [6,7]. To promote the performance of batteries used for hybrid electric vehicles and fuel cell vehicles, it is important to increase the efficiency of research and development efforts by establishing a standardized battery test profile [8]. Until now, there has been little research in this area, and only a few standard test profiles have been proposed for hybrid vehicle batteries. In the Partnership for a New Generation of Vehicles (PNGV) Battery Test Manual among others, Hybrid Pulse Power Characterization (HPPC) test is a part of the listed test procedures. Although the test profile proposed in the HPPC test includes the charge/discharge (C/D) conditions, it cannot represent the transient conditions of hybrid vehicles well, because it requires 1 h of rest between each profile, and each profile contains only one cycle of charging and discharging. Lastly, the main objective of HPPC is to find the power capability, the resistance and the time response constants [9–11]. The second example of a test profile (JEVS D716) is a profile for a cycle life test [8]. Similarly, a cycle life test profile is included in IEC-62660 2010 [12]. Niu proposed a two-condition battery test for hybrid vehicles, one for charging and the other for discharging, that is asymmetric when charging or discharging [13]. In conclusion, these test profiles are unable to simulate the practical operating conditions of hybrid vehicles in some respects, and are thus unable to provide simulation for battery equivalence research.

In this paper, a battery test profile is proposed for hybrid fuel cell buses, and this profile is supported by practical data from road tests. Specifically, the data processed in this paper are accumulated from the three demonstration buses that were recently employed at the 2010 Shanghai World Expo.

This paper is organized as follows: Section 2 introduces the parameters of the three demonstration buses and the control strategy embedded in the vehicle controller. Section 3 explains how the data are processed and the data analysis is presented. Synthesizing the results, Section 4 proposes a test profile for a battery utilized in hybrid PEM fuel cell buses. Section 5 is the result of an experiment using the proposed test profile, while Section 6 provides the discussion and conclusion.

* Corresponding author. Tel.: +86 10 62773437; fax: +86 10 62785708.
E-mail addresses: fxn07@mails.tsinghua.edu.cn (X. Feng), ouymg@tsinghua.edu.cn (M. Ouyang).

0378-7753/$ – see front matter © 2012 Elsevier B.V. All rights reserved.
doi:10.1016/j.jpowsour.2012.02.069

Table 1
Basic parameters of the demonstrated buses [14].

Parameter (Unit)	Value
Vehicle mass with load (t)	14–16
Length (m)	12
Maximum velocity (km h^{-1})	>80
Fuel cell system maximal net power (kW)	80
Battery capacity(A·h)	100
Battery rated voltage (V)	350
Battery minimal voltage (V)	280

2. The demonstration buses and their work modes

2.1. Basic parameters of the demonstration buses

The basic specifications of the demonstration buses at the 2010 Shanghai World Expo are presented in Table 1.

All of the powertrains of the three demonstration buses are the series hybrid structure composed of a PEM fuel cell and Li-ion batteries (Fig. 1).

2.2. Work modes of the fuel cell buses

As seen in Fig. 1, the demonstration buses have the series hybrid structure, which employs four work modes: pure electric mode, joint work mode, braking energy recovery mode and parking charge mode [15].

2.2.1. Pure electric mode

When the motor power requirement is low or the state-of-charge (SOC) of the battery is well over the limit, the power system switches to pure electric mode. This mode also often functions when the bus is running at low speed or moving backward.

2.2.2. Joint work mode

During most road conditions, the bus works in joint work mode. In this mode, the motor drives the bus using the electricity generated by the fuel cell. When the power requirements exceed those that can be provided by the fuel cell, the energy is taken from the battery. When the total system power requirements are low, the excess power from the fuel cell is stored in the battery. In this manner, the fuel cell can always work in its most efficient range.

2.2.3. Braking energy recovery mode

The motor can recycle braking energy to generate electricity, when the bus engages the brakes. This process can turn the kinetic energy of the bus into electric energy for storage in the battery. In addition, the energy recycled tends to be intense. Generally speaking, capturing the recycled energy requires that the batteries efficiently handle pulse currents during charging.

2.2.4. Parking charge mode

When the bus has to be stopped, especially for a prolonged period of time as in a traffic jam, the fuel cell should export electric energy to charge the battery, if the SOC of the battery is very low. This is called parking charge mode. Parking charge mode has distinct advantages over quick charging of the battery and avoids frequent stops of the fuel cell [15].

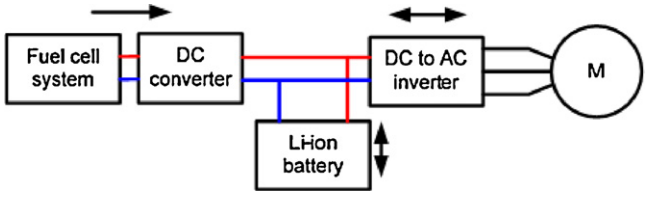

Fig. 1. Structure of the PEM fuel cell/Li-ion battery powertrain. Lines with arrow(s) show the direction of energy flow [13].

2.3. C/D requirements for the battery utilized in hybrid fuel cell buses

The C/D performance depends on both the work modes described above, and the instantaneous SOC of the battery. At this point, it is useful to describe how the control system manages the C/D current. This section will explain in detail when the battery is charged or discharged.

2.3.1. SOC beyond the limits

To manage the safety and life of the battery, the battery management system (BMS) is always monitoring the SOC of the battery. In general, a threshold is pre-set in the BMS to guarantee the battery operates within safe conditions. In a hybrid power system, common thresholds of SOC are 30% and 80% of full charge [15–17]. In addition to considering the safety and life of the battery, another crucial reason for setting such a threshold is to efficiently maintain the power output of the battery utilized in hybrid power system. Once the SOC is below 30%, the battery must stop discharging and turn to charge mode. In contrast, if the SOC is above 80%, the battery must stop charging and turn to pure electric mode.

Except when the SOC is outside the limits, the energy control system of the hybrid bus controls the battery according to the four work modes.

2.3.2. Four work modes

- Pure electric mode: The battery is discharged only.
- Joint work mode: When the output power of the fuel cell exceeds the load, the battery is charged; when the output power of the fuel cell cannot match the load, the battery is discharged.
- Braking energy recovery mode: The battery receives pulse charging.
- Parking charge mode: The battery receives charging under constant voltage and current.

3. Data processing and analysis

3.1. Data processing

From May 2010 to October 2010, the cumulative mileage of the three PEM fuel cell buses demonstrated at the Shanghai World Expo was approximately 10 000 km, as recorded by the data logger. In analyzing the entirety of the data acquired from the demonstration, more attention was paid to data on those that contain complete working conditions including idle, acceleration, cruising, deceleration, braking and parking. Data that contain complete working conditions are defined here as typical data. The typical data were imported into MATLAB, and subsequently transformed into mappings.

3.2. Mapping

The following figures illustrate the demonstration bus data, and are used for further analysis and discussion.

Fig. 2 is a combination of the bus velocity, the voltage of the battery and the C/D current. A negative current indicates charging. This series of figures is used for further discussion in Section 3.4.

Fig. 3 shows the probability density statistics of the C/D current. It is a statistical result acquired from the C/D current data, which is shown in red in Fig. 2.

Fig. 4 is a comparison of the fuel cell output DC/DC power and battery output power. The velocity of the bus is shown as a

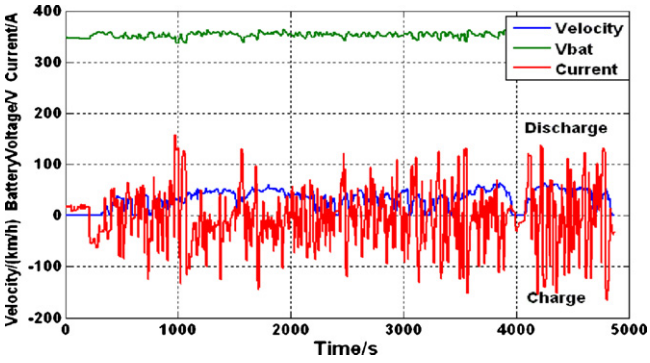

Fig. 2. Bus velocity, battery voltage and current.

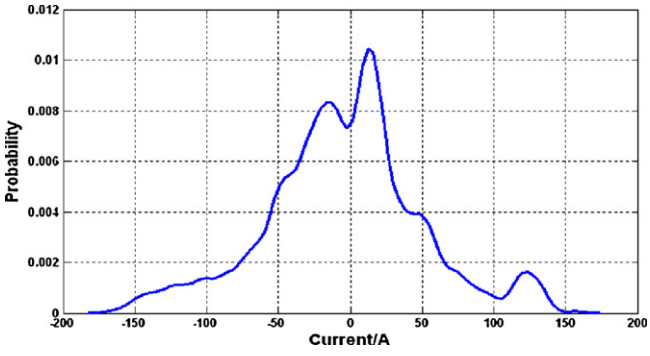

Fig. 3. Probability density of current.

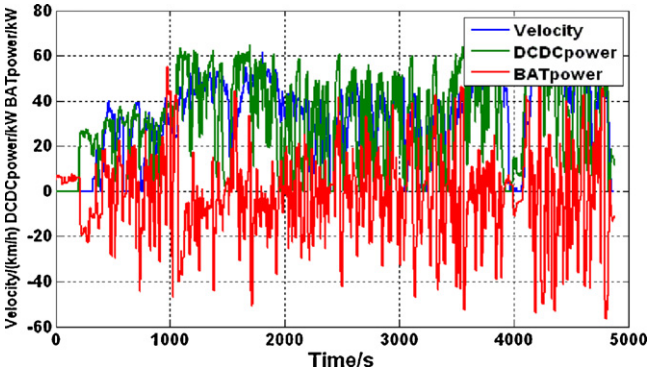

Fig. 4. Fuel cell output DC/DC power in comparison with battery power, and bus velocity.

reference. Figures such as Fig. 4 are used for analysis to characterize the practical operating conditions of the buses.

3.3. Practical conditions

In this section, Fig. 5 is used for power output comparison to generalize the practical operating conditions of the buses. Some of the figures[1] are derived from Fig. 5, while others are selected from other data.

3.3.1. The start-up condition of the buses

Fig. 6 shows the start-up condition of the buses. During the start-up of the buses, the fore-idling fuel cell increases output power directly. The battery no longer absorbs the idle energy generated

[1] To be specific, Fig. 6, Fig. 7, Figs. 9 and 10 are derived from Fig. 5.

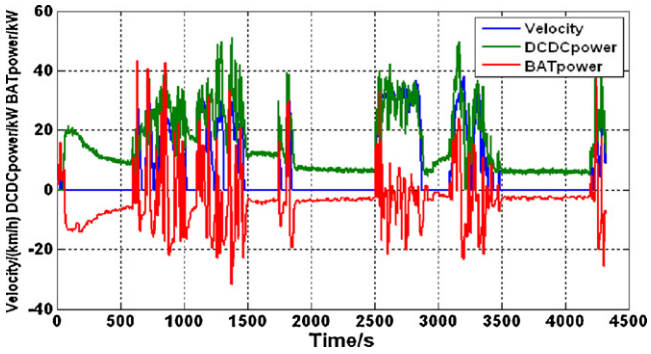

Fig. 5. Schematic diagram used for typical conditions analysis.

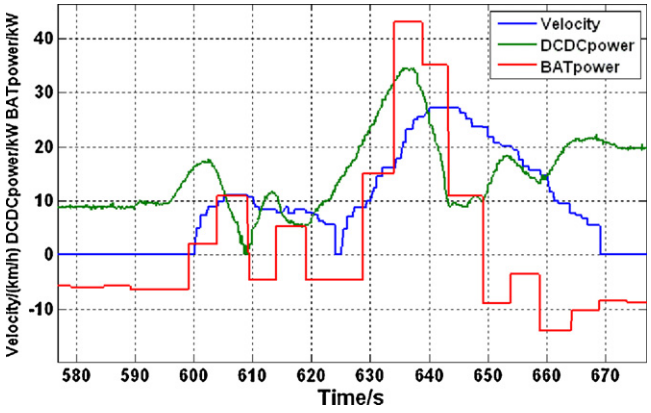

Fig. 6. Start-up condition of the buses.

by the fuel cell. In contrast, it discharges high-level current to compensate the shortage of output power. The output power of the battery pack can even exceed that of the fuel cell.

3.3.2. The idle condition of the buses

Fig. 7 shows the idle condition of the buses. In the idle condition, the buses have zero velocity. Meanwhile, the fuel cell continuously generates power, which is partially absorbed by the battery. The reason for the continuous output of power from the fuel cell is to prevent probable harm to the fuel cell stack caused by frequent start-ups.

3.3.3. The accelerating condition of the buses

Fig. 8 contains many accelerating conditions of the buses. Obviously, no matter what the C/D condition is before the accel-

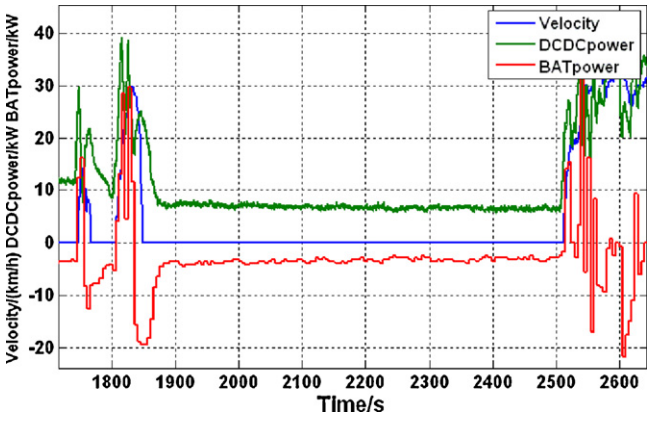

Fig. 7. Idle condition of the buses.

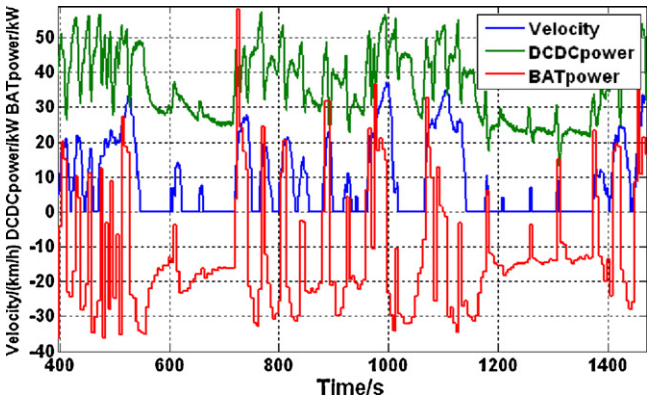

Fig. 8. Accelerating condition of the buses.

erating conditions occur, the battery will switch to discharge once a high current level is required for acceleration.

3.3.4. Cruising and decelerating conditions of the buses

Cruising and decelerating conditions always appear together. Considering the constraints of road traffic, under practical operating conditions, the bus rarely stops. In this condition (Fig. 9), the fuel cell outputs a high level of power continuously to maintain an approximate constant speed with excess power being stored in the battery. Nevertheless, the battery augments output power during some transient accelerating conditions.

3.3.5. The braking condition of the buses

The braking condition is quite common during practical driving conditions. When the bus comes to a bus stop, waits for traffic lights or is obstructed by other vehicles ahead, it has to brake. The deceleration during braking is much greater than the deceleration during cruising condition. As shown in Fig. 10, the battery is charged when the braking condition happens.

3.3.6. The parking conditions of the buses

In the last half of Fig. 11, a typical parking condition is shown. It is quite similar to the idle condition. Moreover, if the fuel cell is shut down when parking, the power to and from the battery should be zero.

3.4. C/D current analysis for practical conditions

In this section, the regulation of the C/D current during practical driving conditions is analyzed with a focus on the magnitude and the conversion frequency of the C/D current.

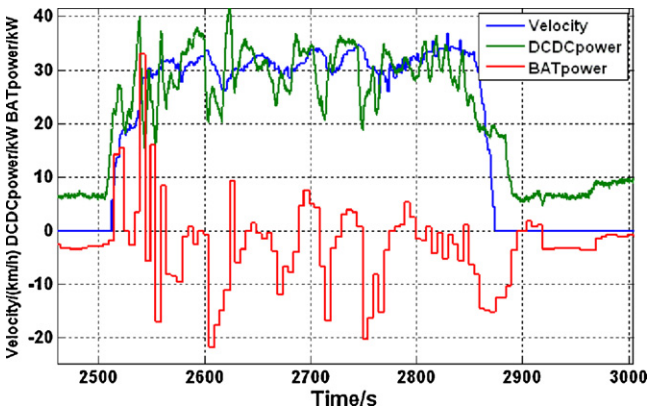

Fig. 9. Cruising and decelerating condition of the buses.

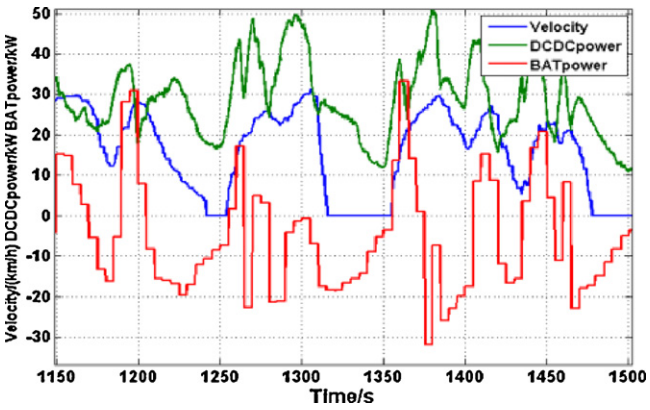

Fig. 10. Braking condition of the buses.

3.4.1. Analysis on the probability density of current

Some common characteristics are found upon analyzing the current density statistics data. These data have been organized into so-called "Three-Ridge" maps. Fig. 12 is a typical Three-Ridge map, and the corresponding current and velocity are provided below. The three ridges represent the charging, idle-parking and the discharging power, respectively.

Other figures can be generalized as deformations of the Three-Ridge map. When the charging condition is more dominant, the "Three-Ridge" map would possibly degrade into a "Two-Ridge" map (Fig. 13). Moreover, when the idle-parking condition occupies most of the time period, the "Three-Ridge" could possibly degrade into a "Single-Ridge" map (Fig. 14), which reflects the low power charging when the bus is idling or parking.

3.4.2. FFT analysis on C/D conversion frequency

Excluding idle-parking condition, i.e., selecting the data of typical Three-Ridge maps (Fig. 12) for analysis, FFT analysis was made on C/D conversion frequency (Fig. 15). As a supplement, the C/D conversion frequency is the frequency that the battery switches from charge to discharge. To be more specific, the conversion frequency of C/D from those practical driving conditions is desired without the interference from idling and parking.

The result of the peak data into frequency must be transformed by

$$\Delta f = \frac{F_s}{N} \tag{1}$$

Δf is the x-axis unit. Here, $F_s = 10$ Hz and $N = 36\,000$, which is determined by the data logger on the fuel cell buses, so that $\Delta f = 10/36\,000 = 1/3600$ Hz.

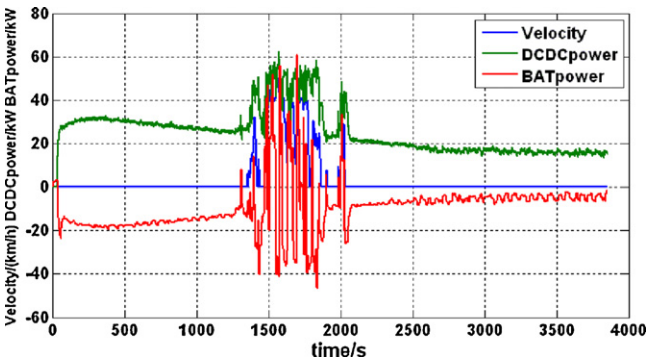

Fig. 11. Parking condition of the buses.

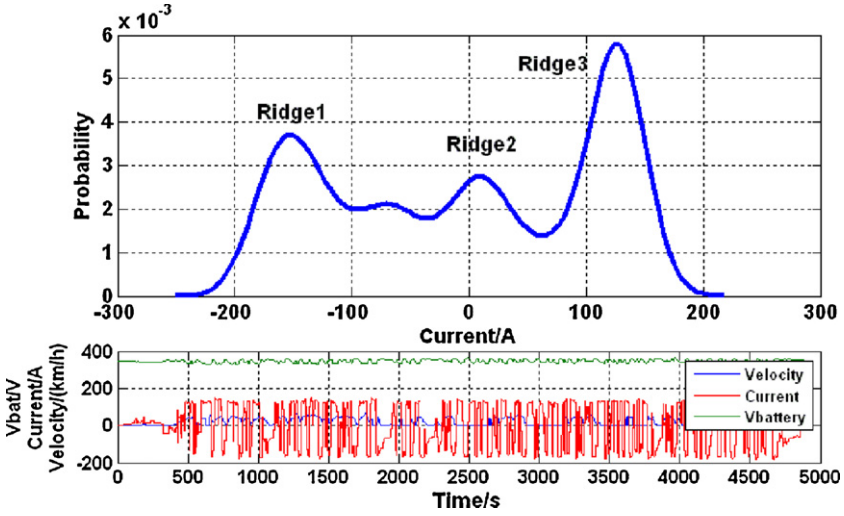

Fig. 12. Typical Three-Ridge map of the probability density of battery current.

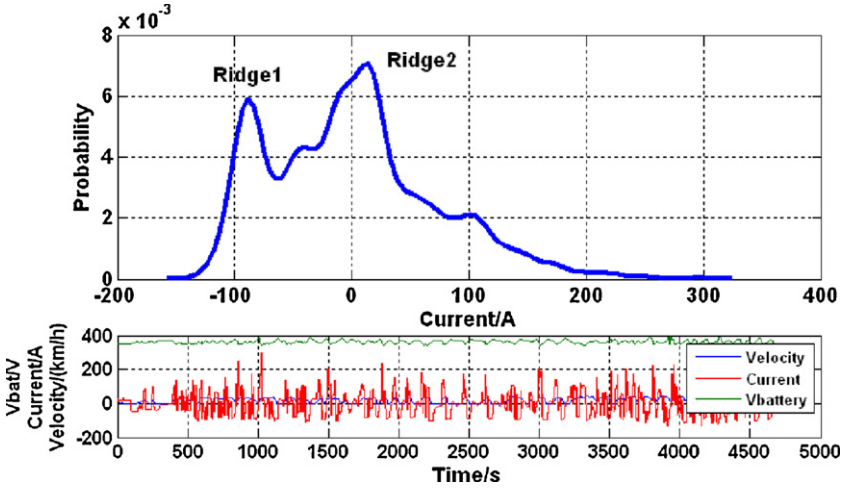

Fig. 13. Degraded Three-Ridge map 1 of the probability density of battery current.

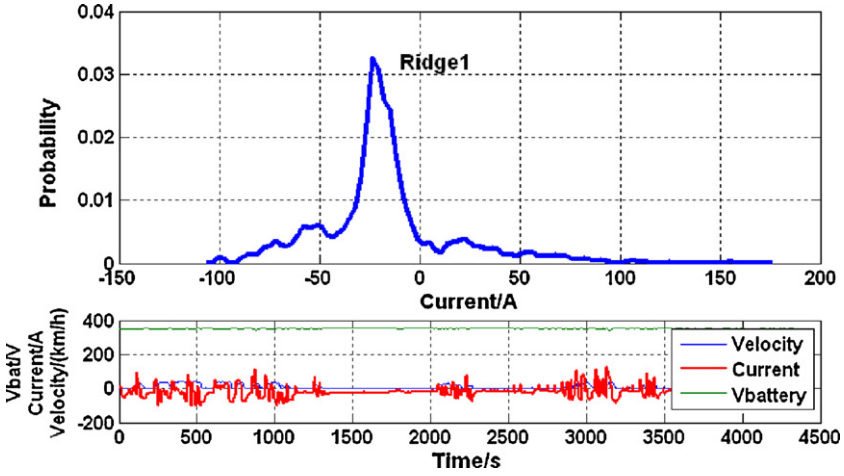

Fig. 14. Degraded Three-Ridge map 2 of the probability density of battery current.

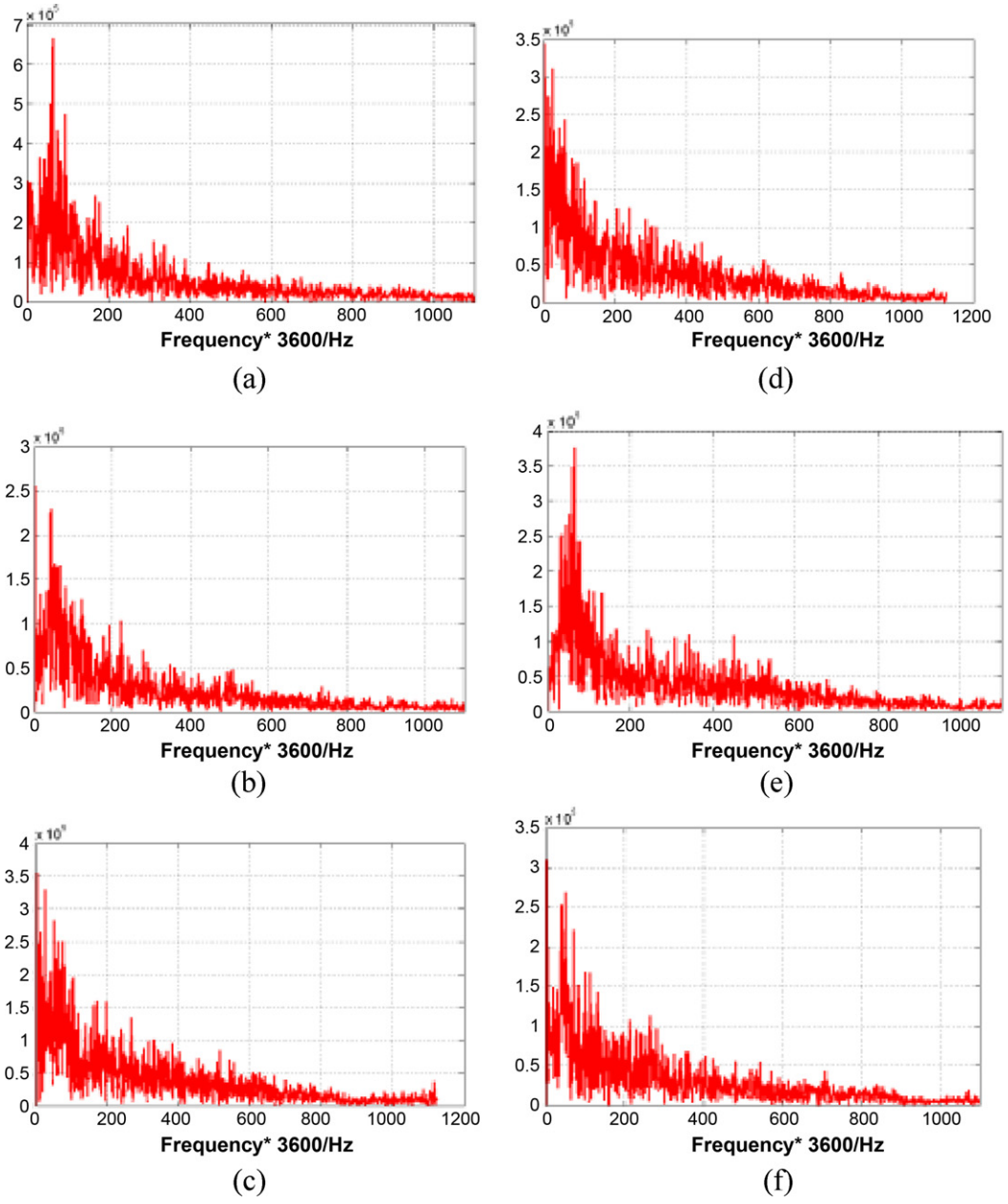

Fig. 15. FFT analysis on C/D conversion time.

After the frequency of C/D conversion is acquired, the time period of C/D conversion can be confirmed by

$$T = \frac{1}{f} \tag{2}$$

In Fig. 15(a), the peak occurs at 64 Hz (at the x-axis label). By Eq. (1), $f = 64/3600$ Hz with Eq. (2) yielding a time period of 56 s.

The result of the FFT analysis can be seen in Table 2. If there are two similar peaks at low frequency, they would be both reserved as reference data.

Table 2
FFT analysis results.

Figure no.	(a)	(b)	(c)	(d)	(e)	(f)
Conversion period (s)	56	138 71	88 80	144 61	56	88 73

The current conversion data is rechecked to confirm the FFT result.

In conclusion, the FFT analysis shows that the C/D conversion period usually occurs within the range of 50 s to 150 s.

3.5. C/D power analysis

Because power is the product of voltage and current, and the battery voltage remains approximately constant, the corresponding power data maps are quite similar to the current data maps. The probability density maps (Fig. 16) of power also show the characteristic "Three-Ridge" structure.

4. Test profile proposed

Based upon the analysis and discussion above, a specific test profile for batteries used in hybrid fuel cell buses is proposed.

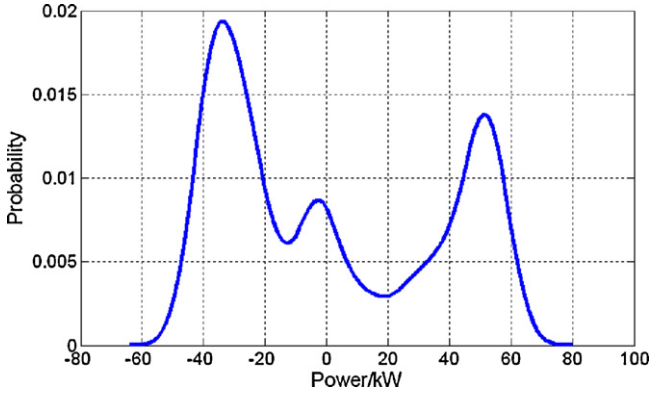

Fig. 16. Probability density of power.

4.1. Composition of test conditions

There are four stages of conditions in the proposed test profile: the calibration, the rest period, the idle-parking condition and the road running condition.

4.2. The calibration

At the beginning of the test, the battery should be fully discharged and then each cell should be charged to the same SOC, e.g., 80%. During this procedure, the BMS can fulfill its calibration of the battery and be well-prepared for the test.

4.3. Idle-parking condition

Referring to the data analyzed in Section 3.3, the idle-parking condition, the battery receives low-level current charging. The specific charging current is in the range of 5–50 A, which follows the output power of the fuel cell. If 30 A is chosen as a test current for the battery of the demonstration buses, that results in 0.3 C of charge for a 100 A-h battery. Finally, a specification named t_{idle} is set here representing the idle-parking time.

4.4. Road running condition

The road running condition component contains the accelerating, cruising, decelerating and braking conditions. The main feature of C/D current during the road running condition is the frequent C/D current conversion.

To set the C/D current in the test profile, the current data statistics from the demonstration buses are analyzed. The effective current data used for C/D current analysis have the characteristic of "Three-Ridge".

Tables 3–5 show part of the statistical results.

As shown in Tables 3–5, the absolute current is usually in a range of 25–150 A. Interestingly, the value tends to be a multiple of 25 A, which is 1/4 C for such a 100 A-h battery. Thus, the C/D currents of the test I_{charge} and $I_{discharge}$, can be set to 1/4 C, 1/2 C, 3/4 C, 1 C, 1.25 C, 1.5 C, etc.

The conversion time of C/D could be determined from the analysis of Section 3.4.2. Here the time period was set to 60 s, exactly 1 min for convenience.

Moreover, the number of C/D conversion cycles N could be set as 10, 20, 30 or 40, etc.

Table 3
Statistic results of peak current in Three-Ridge map of demonstrated bus no. 1.

Bus 1		
Data no.	Charge (A)	Discharge (A)
1	−25	50, 125
2	−50	50
3	−150	125
4	−25	10
5	−30	10

Table 4
Statistic results of peak current in Three-Ridge map of demonstrated bus no. 2.

Bus 2		
Data no.	Charge (A)	Discharge (A)
1	−125	125
2	−50	25
3	−50, −20	50
4	−50, −25	Not obvious
5	−150, −50	100

Table 5
Statistic results of peak current in Three-Ridge map of demonstrated bus no. 3.

Bus 3		
Data no.	Charge (A)	Discharge (A)
1	−75	50, 150
2	−150, −75	25
3	−100	100
4	−60	60
5	−50	75, 150

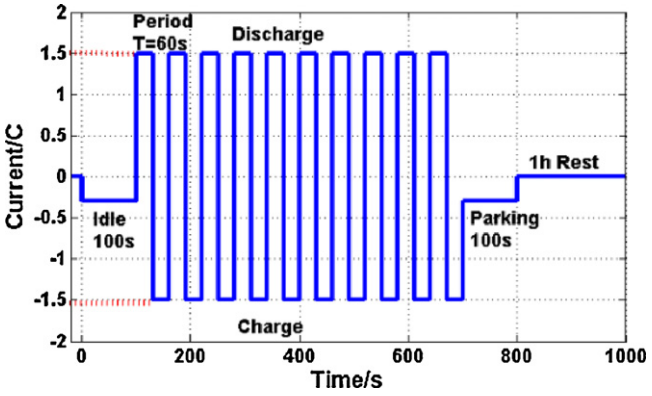

Fig. 17. Road condition test profile for battery.

4.5. Road condition test profile

For the convenience of instruction, the idle-parking condition and road running condition are combined as a whole. The combination is called the road condition test profile (Fig. 17).

The whole procedure of each road condition test profile is defined in Table 6. The values of t_{idle}, I_{charge} and $I_{discharge}$ could be flexible according to needs of practical experiments. Here they are set to 100 s, 1.5 C and −1.5 C, respectively.

Table 6
Parameters about the road condition test profile.

No.	Name	Current (C) rate	Duration (s)
1	Idle	−0.3	100
2	Charge	1.5	30
3	Discharge	−1.5	30
N repetitions of 2 & 3, here *N* = 10			
20	Charge	1.5	30
21	Discharge	−1.5	30
22	Parking	−0.3	100

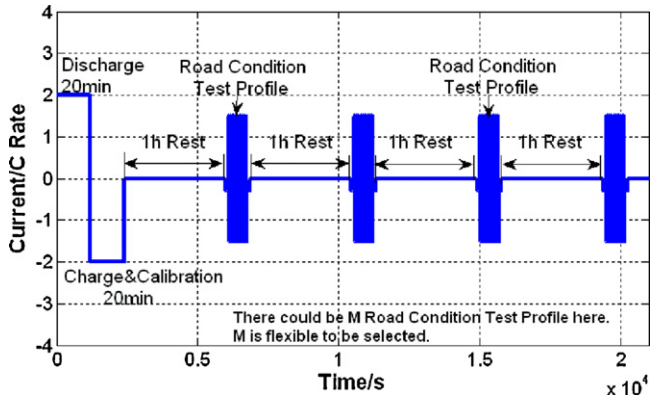

Fig. 18. Complete test profile proposed.

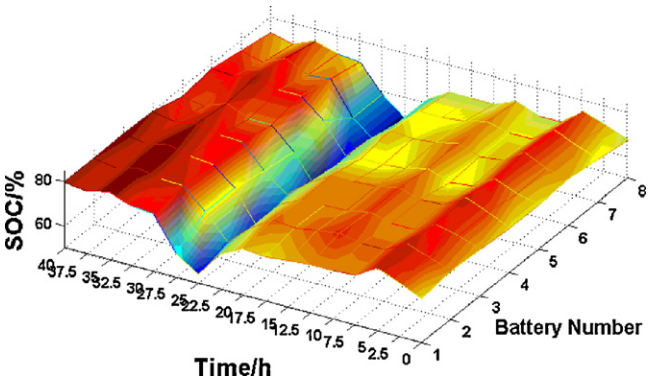

Fig. 20. The result of the experiment.

4.6. The rest period

After calibration and each road condition test profile, the battery rests 1 h to allow the battery to return to an electrochemical and thermal equilibrium condition before applying the next profile.

5. Complete test profile

Comprised of the calibration, the road condition test profile and the rest period, the complete test profile is organized as shown in Fig. 18.

For the completion of a test series, calibration must first be made to prepare for the whole series of tests, where the time of discharge and charge only needs to be approximate, as long as the calibration can be successfully accomplished. Then a rest period follows to assure that the batteries return to their equilibrium conditions. After the rest, a road condition test profile is performed and that can be iterated for M cycles according to the users' requirements. Rests between the M cycles should remain at least 1 h.

6. Experimental results

An experiment on a battery pack consisting of 8 batteries was conducted using the proposed test profile. The batteries are connected in series. After one time calibration at the beginning, an $M = 8$-cycle test on the battery pack. The test process is shown in Fig. 19, where the idle-parking condition is omitted and the C/D current is not strictly symmetric.

The result of the experiment can be seen in Fig. 20. The SOC was evaluated by using the open-circuit-voltage after each rest between cycles.

In addition, the maximum difference of the battery SOC is shown in Fig. 21. Here, the maximum difference is defined as the difference of the maximum SOC and the minimum SOC. It can be seen that the maximum SOC difference is increasing with fluctuations, but the growth rate is very low. After 40 h, the SOC difference has increased by only 2%.

Each battery's maximum SOC difference is shown with the real time mean-value SOC in Fig. 22. Fig. 22(a), (c) and (d) illustrates that the SOCs of the No. 1, No. 3 and No. 4 batteries are offsetting in the positive direction. On the other side, Fig. 22(e), (g) and (h) illustrates that the SOCs of the No. 5, No. 7 and No. 8 batteries are offsetting in the negative direction. This opposing offset causes the increase of the maximum difference of the overall battery pack SOC.

Given that the inconsistency of battery SOCs is increasing, the proposed test profile can be useful for further battery equivalence research.

7. Discussion & conclusion

In this paper a test profile has been proposed for batteries used in hybrid PEM fuel cell buses. This test profile is based on practical data acquired from the demonstration during the 2010 Shanghai World Expo. Such a profile can accurately simulate the practical operating conditions of a hybrid vehicle battery pack and can be used in battery equivalence research.

Here we have a discussion about the methods used in this paper.

First, we filtered large amounts of data. According to the velocity of the buses, we define four work modes of the buses. We believed that data that contain the complete four work modes have the most useful information, thus only those data are used for further analysis.

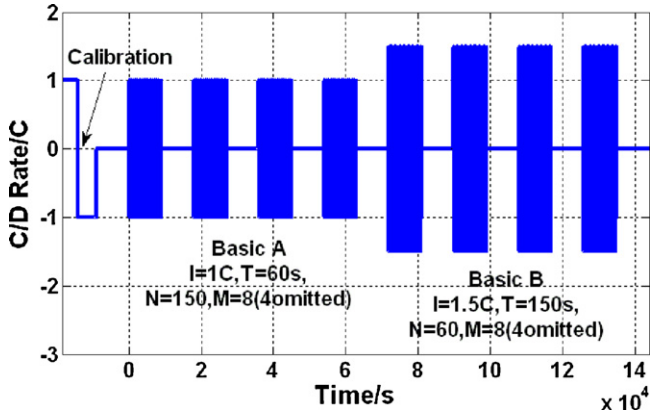

Fig. 19. The experiment test process.

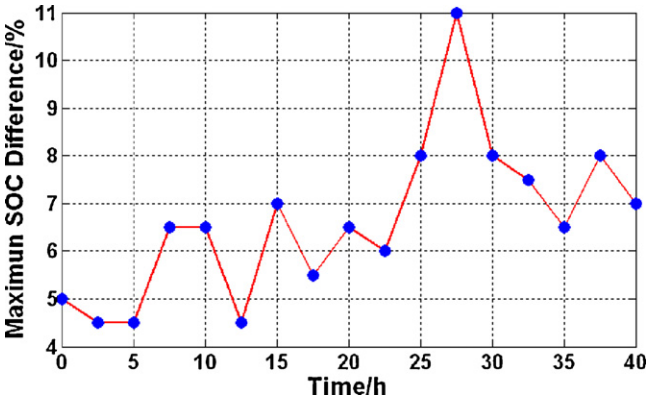

Fig. 21. The maximum difference of the battery SOC.

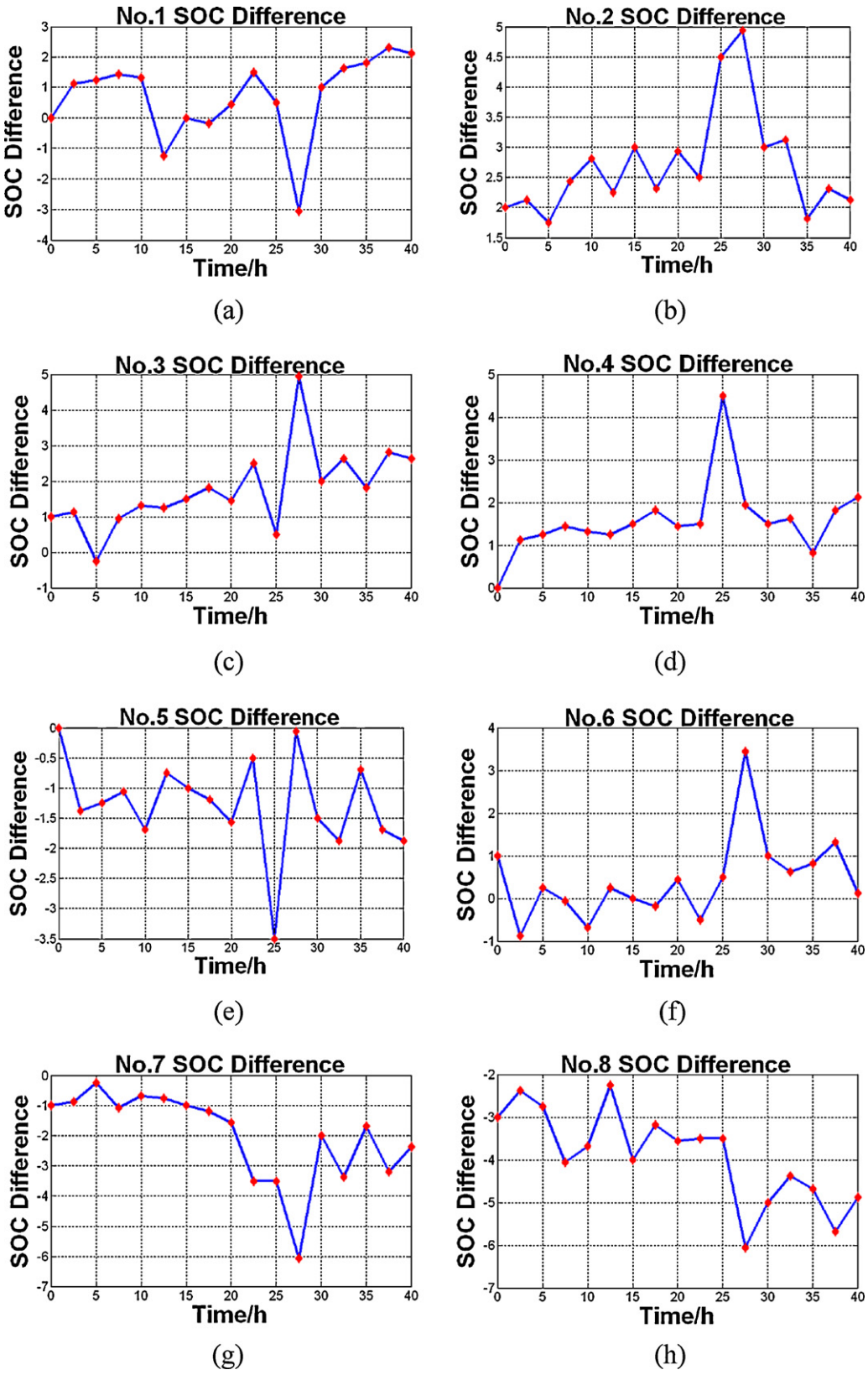

Fig. 22. Each battery's SOC difference with the mean-value SOC.

Second, we use statistical methods to acquire the most common magnitude of the current. It cannot be ignored that the current data in time domain also have statistical significance. At first we introduce histogram to analyze the current data. However, the histogram seems to be not smooth and some information of the current is lost because of the data intervals of the histogram. In addition, we consider the probability density function to describe the current. Then we get the regularity of practical conditions of

hybrid battery, the Three-Ridge maps. It reveals the magnitude of the most common currents. More importantly, the statistical methods can also be used in other analysis of working conditions of electric vehicle.

Third, we apply FFT analysis to get the conversion time of C/D current. In time domain, the current converses frequently as shown in Fig. 12. So we tried to analyze the C/D current in frequency domain. Moreover, the data logger has a stable sampling time, and the data are long enough to apply FFT analysis. The results of FFT analysis reveal the conversion time of C/D current. More importantly, the FFT analysis can not only be applied in this paper, but also be applied in other analysis of electric vehicle, because most data loggers would have stable sampling time.

In conclusion, we believe that the methods used in our data processing would be helpful for other types of electric drive vehicle duty cycles.

Acknowledgments

This work is funded by the MOST (Ministry of Science and Technology) of China under the contract No. 2010DFA72760 and 2011AA11A269, and also supported by the Ministry of Education of the People Republic of China under the contract No. 2010Z08116.

References

[1] C. Fellner, J. Newman, Journal of Power Sources 85 (2000) 229–326.
[2] K.-S. Jeong, W.-Y. Lee, C.-S. Kim, Journal of Power Sources 145 (2005) 319–326.
[3] R.F. Nelson, Journal of Power Sources 91 (2000) 2–26.
[4] J. Larminie, A. Dicks, Fuel Cell Explained, 2nd ed., John Wiley & Sons Ltd, Chichester, 2003, pp. 362–366.
[5] Y. Tang, Y. Wei, M. Pan, Z. Wan, Applied Energy 88 (1) (2011) 68–76.
[6] A. Jonn, B. Andy, S. Kurani Kenneth, Batteries for Plug-in Hybrid Electric Vehicles (PHEVs): Goals and the State of Technology circa 2008, Institute of Transportation Studies, UC Davis, 2008.
[7] D. Linden, T.B. Reddy, Handbook of Batteries, 3rd ed., McGraw-Hill Companies, Inc., NY, 2002, p. 724 (in Chinese).
[8] K. Morita, M. Akai, H. Hirose, 24th International Electric Vehicle Symposium and Exposition (EVS-24), Stavanger, Norway, May 13–16, 2009.
[9] PNGV Battery Test Manual, 2001, pp. 3–7.
[10] Freedom CAR Battery Tests Manual for Power-Assist Hybrid Electric Vehicles, 2003, pp. 3–7.
[11] Battery Test Manual for Plug-in Hybrid Electric Vehicles, Idaho National Laboratory, 2008, pp. 5–8.
[12] IEC-62660-1, Edition 1.0, 2010–12, pp. 23–26.
[13] M. Niu, Ms D Thesis, Beijing Jiaotong University, Beijing, June 2010, pp. 43–46.
[14] L. Xu, M. Ouyang, J. Li, J. Hua, The 25th World Battery, Hybrid and Fuel Cell Electric Vehicle Symposium and Exposition (EVS-25), Shenzhen, China, November 5–9, 2010.
[15] M. Ouyang, J. Li, F. Yang, L. Lu, Automotive New Powertrain: Systems, Models and Controls, Tsinghua University Press, Beijing, 2008, pp. 261–281, 329.
[16] B. Wang, Z. Xu, Modern Electronics Technique (2009) 168–170 (in Chinese).
[17] M. Niu, J. Jiang, H. Guo, Microprocessors (2010) 125–127 (in Chinese).